Fingerprints of Anti-Pfaffian Topological Order in Quantum Point Contact Transport

Jinhong Park[1,2] Christian Spånslätt,[3] and Alexander D. Mirlin[1,2]

[1]*Institute for Quantum Materials and Technologies, Karlsruhe Institute of Technology, 76131 Karlsruhe, Germany*
[2]*Institut für Theorie der Kondensierten Materie, Karlsruhe Institute of Technology, 76131 Karlsruhe, Germany*
[3]*Department of Microtechnology and Nanoscience (MC2), Chalmers University of Technology, S-412 96 Göteborg, Sweden*

Despite recent experimental developments, the topological order of the fractional quantum Hall state at filling $\nu = 5/2$ remains an outstanding question. We study conductance and shot noise in a quantum point contact device in the charge-equilibrated regime and show that, among Pfaffian, particle-hole Praffian, and anti-Pfaffian (aPf) candidate states, the hole-conjugate aPf state is unique in that it can produce a conductance plateau at $G = (7/3)e^2/h$ by two fundamentally distinct mechanisms. We demonstrate that these mechanisms can be distinguished by shot noise measurements on the plateaus. We also determine distinct features of the conductance of the aPf state in the coherent regime. Our results can be used to experimentally single out the aPf order.

Introduction.—The fractional quantum Hall (FQH) state at filling $\nu = 5/2$ [1] is the prototypical candidate for a non-Abelian phase of matter [2]. This state has attracted immense attention as a tentative platform for topological quantum computations [3]. However, to experimentally verify the realized topological order at this filling remains an outstanding problem in condensed-matter physics [4,5].

To describe the $\nu = 5/2$ state, several candidate states were proposed, most prominently the Pfaffian (Pf) [2], anti-Pfaffian (aPf) [6,7] and particle-hole Pfaffian (phPf) states [8–11] (see also a related state in Ref. [12]), all with non-Abelian orders. To date, numerical simulations favor either the aPf or Pf state [13–18], while in GaAs/AlGaAs devices, recent measurements of the thermal conductance [19–21] and upstream noise [22] point towards the phPf state, supported by edge theory [23–25]. Moreover, despite recent observations of several even-denominator states in novel 2D materials [26–33], detailed transport experiments at $\nu = 5/2$ in these materials remain elusive.

In this Letter, we address the $\nu = 5/2$ conundrum by analyzing edge transport through a quantum point contact (QPC) device. Our main goal is to identify hallmarks of the aPf order related to its hole-conjugate nature, i.e., the presence of *counterpropagating* edge modes. In the regime of equilibrated charge transport, the aPf state is expected to display a highly nontrivial plateau in the two-terminal conductance, $G = 7/3$ (in units of e^2/h), when the QPC is continuously tuned by a gate voltage. This plateau arises when the local QPC filling factor is $\nu_{\rm QPC} = 3$ [Fig. 1(a)], i.e., *higher* than the bulk filling $\nu_B = 5/2$, see Ref. [34] for a discussion of related quantum-dot and line-junction setups. Among the non-Abelian candidates, this exotic mechanism of plateau formation is operative only for the aPf state due to its unique hole-conjugate character.

However, a $G = 7/3$ plateau may form by another mechanism for *any* $\nu = 5/2$ candidate state. This happens if the QPC instead *lowers* the local density to the stable FQH filling $\nu_{\rm QPC} = 7/3$, i.e., for $\nu_{\rm QPC} < \nu_B$ [35]. We demonstrate that these two kinds of $G = 7/3$ plateaus can be distinguished by on-plateau shot noise measurements, which thereby provide a unique fingerprint for the aPf state. Further, we explore the evolution of the $G = 7/3$ plateau arising from $\nu_{\rm QPC} = 3$ in the aPf state in the regime of coherent charge transport, which can be reached for the lowest temperatures and bias voltages. We show that, due to disorder, G then generically fluctuates with changing QPC gate voltage within the range $35/17 \leq G \leq 3$. Among the three non-Abelian candidate states, $G > 5/2$ is reachable
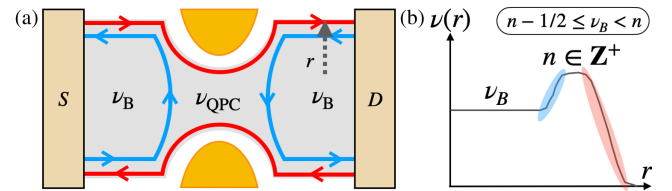

FIG. 1. (a) Schematic setup to measure the two-terminal conductance $G \equiv I/(V_S - V_D)$ across a quantum point contact (QPC) in the FQH regime. Here, I is the current collected in drain (D), and V_S and V_D are the source (S) and drain voltages, respectively. For a hole-conjugate state, the QPC region can accommodate a FQH liquid with local filling $\nu_{\rm QPC}$ *higher* than the bulk filling factor ν_B. Red and blue solid lines with arrows depict counterpropagating edge modes. (b) Sketch of the local filling factor $\nu(r)$ along the gray dashed line in (a). Because of the hole-conjugate nature of the edge, there exists a region with higher, integer filling $n > \nu_B$. Red and blue jumps in $\nu(r)$ correspond to the edge modes in (a).

only for the aPf state, which provides a complementary fingerprint of this topological order.

QPC conductance plateaus.—The unusual situation with $\nu_{QPC} > \nu_B$ is a feature common to all hole-conjugate states, i.e., for fillings satisfying $n - 1/2 \leq \nu < n$, with $n \in \mathbb{Z}^+$. Indeed, all such states can be viewed as FQH liquids formed by condensation of holelike quasiparticles on top of an integer number n of filled Landau levels [36–38]. As a consequence, hole-conjugate states naturally accommodate local regions with $\nu(r) = n > \nu_B$ [see Fig. 1(b)]. This property suggests the possibility of a local region with integer-valued filling $\nu_{QPC} = n$, despite the application of a negative gate voltage that normally *lowers* the local density. Having $\nu_{QPC} > \nu_B$, together with the assumption of fully equilibrated charge transport, leads to nontrivial conductance plateaus [39]

$$G = \frac{\nu_B \nu_{QPC} - (2\nu_B - \nu_{QPC})\nu_T}{2\nu_{QPC} - \nu_B - \nu_T}, \quad \text{for } \nu_{QPC} > \nu_B, \quad (1)$$

see Fig. 1(a) for the schematic QPC setup. Here, ν_T is the total filling factor discontinuity associated with fully transmitted modes (without any coupling to the other modes). Equation (1) explains recently observed conductance plateaus for hole-conjugate FQH states [43–45]. In particular, for the $\nu_B = 2/3$ state (with $\nu_{QPC} = 1$ and $\nu_T = 0$), a $G = 1/2$ plateau was recently observed [43,44]. Also FQH states in higher Landau levels were observed to display nontrivial plateaus classified by Eq. (1) [45].

Crucially, among the $\nu = 5/2$ candidate states, it is only the aPf state that is hole conjugate. Hence, only the aPf can produce a conductance plateau by the mechanism governing Eq. (1). For $\nu_B = 5/2$, $\nu_T = 2$, and $\nu_{QPC} = 3$, Eq. (1) evaluates to $G = 7/3$, in agreement with Ref. [34].

However, conductance plateaus may also arise for a reduced density in the QPC region [35], with

$$G = \nu_{QPC}, \quad \text{for } \nu_{QPC} < \nu_B. \quad (2)$$

In contrast to the plateaus (1), Eq. (2) holds for any FQH state provided that the state with filling $\nu_{QPC} < \nu_B$ is stabilized in the QPC region. Experimental observations of plateaus for various FQH states [46–48] can be attributed to this mechanism. We see that, according to Eq. (2), the value $G = 7/3$ is also generated for $\nu_B = 5/2$ regardless of the bulk topological order if the QPC region hosts a $\nu_{QPC} = 7/3$ FQH state. Such a state is indeed the most prominent state in the range $2 < \nu < 5/2$. Hence, to differentiate the two distinct types of $7/3$ plateaus and thus to find unique fingerprints for the aPf state, complementary measurements are needed. We will show that on-plateau shot noise measurements meet this demand.

APf edge theory.—The edge consists of three modes in the second Landau level: two counterpropagating bosonic modes ϕ_1 (red solid lines in Fig. 2) and $\phi_{\frac{1}{2}}$ (blue solid lines)

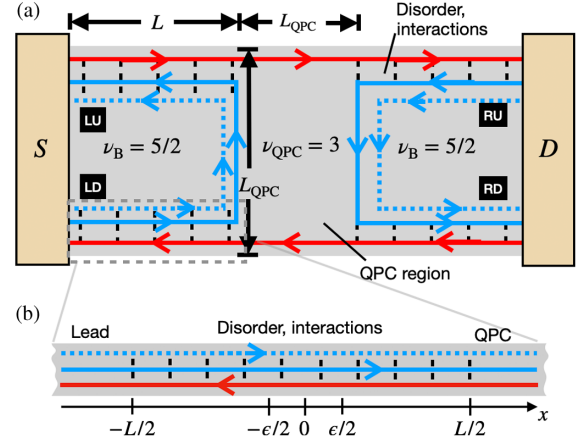FIG. 2. (a) QPC configuration for the anti-Pfaffian state with QPC filling stabilized at $\nu_{QPC} = 3$. Red and blue solid lines depict $\delta\nu = 1$ and $\delta\nu = -1/2$ edge modes propagating in the opposite directions. The dashed blue line depicts a Majorana mode propagating in the same direction as the $\delta\nu = -1/2$ mode. The edge modes are coupled by disorder-induced scattering in each individual arm of the QPC. The two fully transmitted integer modes in the lowest Landau levels are not shown. (b) Enlargement of one QPC arm which bridges the interaction and disorder-free lead region ($x < -L/2$) and the QPC region ($x > L/2$). All impact of disorder is accounted for by the narrow region $|x| < \epsilon/2$ with $\epsilon \to 0^+$. This feature holds for all four arms LU, LD, RU, and RD in (a).

associated with the filling factor discontinuities $\delta\nu = 1$ and $\delta\nu = -1/2$, respectively, as well as one charge-neutral Majorana mode $\chi = \chi^\dagger$ (blue dashed lines) [6,7]. We disregard two integer modes of the lowest Landau levels, assuming that they are decoupled and simply give a contribution 2 to G. The edge action is $S = \int dt(\mathcal{L}_0 + \mathcal{L}_{dis})$ with

$$\mathcal{L}_0 = \int \frac{dx}{4\pi} \left[\left(-\partial_x \phi_1 (\partial_t + v_1 \partial_x) \phi_1 + 2\partial_x \phi_{\frac{1}{2}} (\partial_t - v_{\frac{1}{2}} \partial_x) \phi_{\frac{1}{2}} \right. \right.$$
$$\left. - 2v_{int} \partial_x \phi_1 \partial_x \phi_{\frac{1}{2}} \right) - i\chi(\partial_t - v_M \partial_x)\chi \right],$$
$$\mathcal{L}_{dis} = -\frac{1}{\sqrt{2\pi a}} \int dx \chi(x) \left(\xi(x) e^{i(\phi_1 + 2\phi_{\frac{1}{2}})} - \text{H.c.} \right). \quad (3)$$

Here, v_1, $v_{\frac{1}{2}}$, and v_M are the mode speeds, v_{int} is the intermode interaction strength, and a is an ultraviolet length cutoff. The term $\mathcal{L}_{dis}$ describes disorder-induced electron tunneling with the random complex amplitude $\xi(x)$. The scaling dimension of the disorder term evaluated with respect to $\mathcal{L}_0$ is $\Delta = 1/2 + (3/2 - 2x)/\sqrt{1 - 2x^2}$, where $x = v_{int}/(v_1 + v_{\frac{1}{2}})$.

When $\mathcal{L}_{dis}$ is relevant in the renormalization group (RG) sense for $\Delta < 3/2$ [49], the edge is driven to a disordered fixed point where $\Delta = 1$ [6,7]. At this point, the edge hosts three decoupled modes: one charge mode
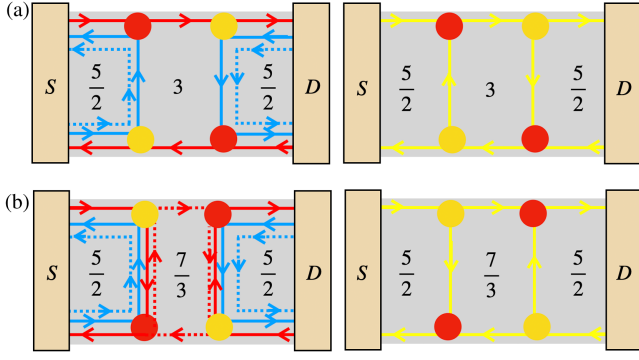
FIG. 3. Hot spots (red regions) and noise spots (yellow regions) for the two distinct $G = 7/3$ plateaus of the aPf state in the incoherent regime: (a) $\nu_{\mathrm{QPC}} = 3 > \nu_B = 5/2$ and (b) $\nu_{\mathrm{QPC}} = 7/3 < \nu_B$. Left panels: the edge configurations. Right panels: the charge flow (yellow, solid lines) along each edge segment.

$\phi_c \equiv \sqrt{2}(\phi_1 + \phi_{\frac{1}{2}})$, one neutral mode $\phi_n \equiv \phi_1 + 2\phi_{\frac{1}{2}}$, and the remaining Majorana mode χ. These are described by $\mathcal{L}_{\mathrm{fix}} = \mathcal{L}_c + \mathcal{L}_n$, where

$$\mathcal{L}_c = \int \frac{dx}{4\pi}[-\partial_x \phi_c(\partial_t + v_c \partial_x)\phi_c],$$

$$\mathcal{L}_n = \int dx \left[\frac{1}{4\pi}\partial_x \phi_n(\partial_t - \bar{v}_n \partial_x)\phi_n - i\chi(\partial_t - \bar{v}_n \partial_x)\chi \right.$$
$$\left. - \frac{1}{\sqrt{2\pi a}}\left(\xi(x)e^{i\phi_n} - \text{H.c.} \right)\chi \right]. \quad (4)$$

Near the fixed point, all possible terms (e.g., $\phi_c - \phi_n$ interactions and the velocity anisotropy) are RG irrelevant [6,7]. Still, these terms cause decoherence, which leads to intermode equilibration governed by the characteristic charge equilibration length $\ell_{\mathrm{eq}}^c \sim T^{-2}$, with T the temperature. This length defines two distinct charge transport regimes: the *coherent* regime $L \ll \ell_{\mathrm{eq}}^c$ and the *incoherent* regime $L \gg \ell_{\mathrm{eq}}^c$. L denotes the length of the arms of the QPC (see Fig. 2). In the following, we separately discuss transport properties in these two regimes.

Shot noise in the incoherent regime.—We now show that the two types of $G = 7/3$ plateaus for the aPf generate very distinct (dc) shot noise characteristics as they correspond to two distinct QPC configurations: (i) $\nu_{\mathrm{QPC}} = 3 > \nu_B = 5/2$ in Fig. 3(a) and (ii) $\nu_{\mathrm{QPC}} = 7/3 < \nu_B$ in Fig. 3(b). Measurements of nonequilibrium noise involving (partial) equilibration on edge segments were recently proposed and experimentally implemented as a versatile tool to probe the topological order in various FQH setups [20,23–25,35,50–56].

The on-plateau shot noise generated in the process of equilibration (a hallmark of the incoherent regime) among counterpropagating edge modes depends on the competition of several characteristic length scales. We therefore first establish the relevant hierarchy of these length scales.

Motivated by recent experimental observations in both GaAs/AlGaAs and graphene devices, we assume

$$\ell_{\mathrm{eq}}^c \ll L_{\mathrm{QPC}} \ll \ell_{\mathrm{eq}}^h \ll L. \quad (5)$$

Here, ℓ_{eq}^h is the heat equilibration length and L_{QPC} is the size of the QPC region [see Fig. 2(a)]. While full charge equilibration is achieved over a very short scale ($\lesssim 1$ μm) in essentially all FQH devices (see, however, Refs. [57–60] for prominent exceptions), heat equilibration is often poor at low temperatures with $\ell_{\mathrm{eq}}^h \sim 100$ μm [20,52,53,61–66]. We also assume no edge reconstruction, based on recent measurements of the thermal conductance in graphene [64–66], which remarkably agree with the values for thermally nonequilibrated transport without edge reconstruction. This is further corroborated by scanning tunneling microscopy experiments [67].

The mechanism for on-plateau shot noise generation in the incoherent regime is due to charge partitioning at "noise spots" (yellow regions in Fig. 3) [23,35,50,51]. An intermode charge tunneling event contributes to the noise only if the constituents of the resulting particle-hole pair reach different contacts S and D. This indeed happens only at the noise spots, where the charge current partitions into these contacts, see the right panels in Fig. 3 for depictions of the charge flows (solid, yellow lines). Importantly, the tunneling processes in each noise spot are dominantly generated by an increase of the noise spot temperature. This heating occurs by heat flowing from hot spots (red regions in Fig. 3), where all Joule heating occurs, to the noise spots. The generated noise in a noise spot, S_{NS}, given by

$$S_{\mathrm{NS}} = \frac{e^2}{h}\frac{(\nu_d - \nu_u)\nu_u}{\nu_d} k_B(T_d + T_u). \quad (6)$$

Here, $\nu_{d/u} = \sum_{n=1}^{n_{d/u}} \delta\nu_{d/u,n}$ is the total filling factor discontinuity of the charged modes propagating downstream and upstream, respectively, and n_d and n_u denote the number of charged downstream and upstream modes, respectively. Furthermore, $T_{d/u}$ is the temperature of all downstream and upstream modes at the noise spot. To compute the total noise in the drain D, we calculate the local temperatures at the noise spots by solving a set of transport equations for the charge and energy current along each edge segment on suitable boundary conditions at the contacts; see Supplemental Material [39].

In configuration (i), for the experimentally relevant length hierarchy (5), we obtain $k_B T_d = \sqrt{5/6}eV/\pi$ and $k_B T_u = \sqrt{5}eV/(3\pi)$. Then, the noise S measured in the drain D is given by

$$S = \frac{8S_{\mathrm{NS}}}{9} = \frac{8e^3(\nu_d - \nu_u)\nu_u}{9h\nu_d}k_B(T_d + T_u) \approx \frac{0.12e^3V}{h}, \quad (7)$$

upon substituting $\nu_d = 1$, $\nu_u = 1/2$ for the aPf state. The prefactor 8/9 stems from the conversion of the single noise
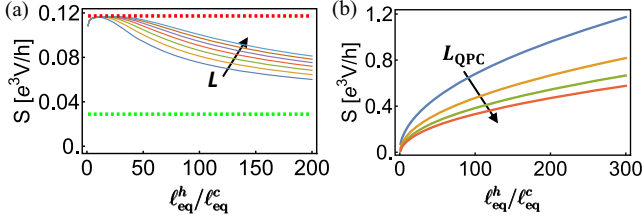
FIG. 4. Anti-Pfaffian noise characteristics S (in units of e^3V/h where V is the bias voltage) vs the ratio of heat and charge equilibration lengths $\ell_{\mathrm{eq}}^h/\ell_{\mathrm{eq}}^c$. The noise is evaluated for the two different QPC configurations in Fig. 3. (a) S is plotted for $\nu_{\mathrm{QPC}} = 3 > \nu_B = 5/2$. The solid lines correspond to different choices of QPC arm lengths $200 \leq L/\ell_{\mathrm{eq}}^c \leq 500$ in steps of 50. The red and green dashed lines correspond to analytical values obtained for the hierarchy (5), and in the limit $\ell_{\mathrm{eq}}^c \ll L \ll \ell_{\mathrm{eq}}^h$, respectively. (b) S is computed for $\nu_{\mathrm{QPC}} = 7/3 < \nu_B$ for different L_{QPC}, $3 \leq L_{\mathrm{QPC}}/\ell_{\mathrm{eq}}^c \leq 12$ in steps of 3, with fixed $L = 300\ell_{\mathrm{eq}}^c$.

spot S_{NS} to the total noise S [39]. In Fig. 4(a), we plot S vs the ratio $\ell_{\mathrm{eq}}^h/\ell_{\mathrm{eq}}^c$ for different choices of L. For relatively small $\ell_{\mathrm{eq}}^h/\ell_{\mathrm{eq}}^c$, S approaches Eq. (7), as indicated by the red, dashed line. Further increasing $\ell_{\mathrm{eq}}^h/\ell_{\mathrm{eq}}^c$ causes S to monotonously decrease towards $S \approx 0.029e^3V/h$ (green, dashed line), the value in the regime of vanishing thermal equilibration in the QPC arms, $\ell_{\mathrm{eq}}^h \gg L$ [39]. As L increases, the region of Eq. (7) broadens, which reflects that ℓ_{eq}^h satisfies the hierarchy (5) for a broader range of values.

In configuration (ii), we find instead $S \propto \sqrt{\ell_{\mathrm{eq}}^h/L_{\mathrm{QPC}}}$ for the hierarchy (5), where S increases with increasing ℓ_{eq}^h in contrast to Eq. (7) [see Fig. 4(b)]. This behavior results from an emergent, circulating $\delta\nu = 1/3$ mode in the QPC region [see Fig. 3(b)]. This mode heats up continuously by Joule heating at the hot spots until the heat escapes to other edge modes by thermal equilibration. The circulating heat current effectively winds $\sim \ell_{\mathrm{eq}}^h/L_{\mathrm{QPC}}$ times before it reaches a steady state, and as a result, T_d, T_u, and S scale as $\sqrt{\ell_{\mathrm{eq}}^h/L_{\mathrm{QPC}}}$. Crucially, regardless of the topological order of the $\nu = 5/2$ states, the $\delta\nu = 1/3$ mode always exists in configuration (ii), and therefore this type of noise characteristics holds for all $\nu = 5/2$ candidate states (including Abelian states).

Conductance in the coherent regime.—At sufficiently low temperatures and voltages, FQH experiments can reach the regime where the charge equilibration is weak [58–60]. In this regime for the aPf state, each QPC arm segment is described by the fixed point Lagrangian (4). The neutral sector $\mathcal{L}_n$ has an emergent SO(3) symmetry [6,7]: by defining the Majorana mode triplet $\psi^T \equiv (\psi_1, \psi_2, \psi_3)$ with $\psi_1 = (1/2\sqrt{\pi a})(e^{i\phi_n} + e^{-i\phi_n})$, $\psi_2 = [(-i)/2\sqrt{\pi a}](e^{i\phi_n} - e^{-i\phi_n})$ and $\psi_3 = \chi$, we express $\mathcal{L}_n$ as

$$\mathcal{L}_n = \int_{x \in \mathcal{R}_{\mathrm{Arm}}} dx \left[-i\psi^T \left(\partial_t - \bar{v}_n \partial_x + \sum_{a=1,2} \xi_a \hat{L}_a \right) \psi \right]. \quad (8)$$

Here, $\xi_1 \equiv \mathrm{Re}(\xi)$, $\xi_2 \equiv -\mathrm{Im}(\xi)$ and $(\hat{L}_a)_{bc} \equiv \epsilon_{abc}$ are the generators of SO(3). The integration range in Eq. (8) includes all four arm regions in the QPC, $x \in \mathcal{R}_{\mathrm{Arm}}$; i.e., the regions $|x| < L/2$ in Fig. 2(b). In contrast, the disorder-free lead and QPC regions are described by the clean $\mathcal{L}_0$ in Eq. (3). With a suitable orthogonal transformation $\tilde{\psi}(x) = U^T(x)\psi(x)$, Eq. (8) becomes

$$\mathcal{L}_n = \int_{x \in \mathcal{R}_{\mathrm{Arm}}} dx [-i\tilde{\psi}^T (\partial_t - \bar{v}_n \partial_x)\tilde{\psi}]$$
$$- \frac{2i\theta\bar{v}_n}{\sqrt{\pi a}} \sin(\phi_n(x=0))\chi(x=0). \quad (9)$$

Here θ is a Euler angle to characterize a rotation around the $\hat{x}$ axis on SO(3) space for $\psi(x)$; see Supplemental Material [39] for more details on the transformation. We see that the action (9) has two fixed points, which correspond to the two values of $\theta = 0, \pi$, where disorder can be fully removed. While $\theta = 0$ directly removes the disorder in Eq. (9), for $\theta = \pi$, the θ term can be gauged away upon substituting $\phi_n \to -\phi_n$ and $\chi \to -\chi$ in the region $x > L/2$. Equivalently, in a picture of a Bloch sphere on which ψ rotates by evolving with $U(x)$, ψ does not rotate at all for $\theta = 0$ (clean limit), while ψ rotates from the north to the south pole or vice versa for $\theta = \pi$. A detailed RG analysis for the entire device shows that $\theta = 0$ and $\theta = \pi$ correspond to a stable and unstable fixed point, respectively [39].

With the two possible fixed points at hand, we determine the coherent two-terminal conductance G in Fig. 2. To this end, we boundary match ϕ_n and ϕ_c on all interfaces between lead and arm regions as well as between QPC regions and arm regions [39]. For all possible combinations of arm fixed points (i.e., for $\theta_{ij} = 0$ or $\theta_{ij} = \pi$ with labels $i \in \{\mathrm{L(left)}, \mathrm{R(right)}\}$ and $j \in \{\mathrm{U(up)}, \mathrm{D(down)}\}$), we find

$$G = \begin{cases} 2 + \frac{1}{17} & \text{for all } \theta_{ij} = \pi, \\ 2 + \frac{1}{9} & \text{for } \theta_{\mathrm{LU}} = \theta_{\mathrm{LD}} = \pi \text{ and } \theta_{\mathrm{RU}} \cdot \theta_{\mathrm{RD}} = 0, \\ & \text{or } \theta_{\mathrm{RU}} = \theta_{\mathrm{RD}} = \pi \text{ and } \theta_{\mathrm{LU}} \cdot \theta_{\mathrm{LD}} = 0, \\ 2 + 1 & \text{otherwise.} \end{cases} \quad (10)$$

Here, 2 represents the contribution of the two lowest-Landau-level integer modes. At sufficiently low T, such that $L < L_T \equiv \hbar v_n/T$, each arm region is separately driven to the $\theta_{ij} = 0$ fixed point. In this clean device regime, the conductance is maximal at $G = 3$. In contrast, for $L_T < L < \ell_{\mathrm{eq}}^c$, G fluctuates and its value depends on the specific disorder realizations, i.e., the precise values of all θ_{ij}. These fluctuations generically range between $G = 2 + 1/17$ ($\theta_{ij} = \pi$) and $G = 3$. As L exceeds ℓ_{eq}^c (i.e., the

incoherent regime), G approaches $G = 2 + 1/3$ as discussed above.

We emphasize that, due to its unique hole-conjugate nature, the aPf edge permits upstream charge transport, allowing $G > \nu_B = 5/2$ in the coherent regime. By contrast, the Pf and phPf edges do not entail upstream charge transport (assuming no edge reconstruction), so that G cannot exceed $5/2$. Hence, $G > 5/2$ in the QPC geometry is a hallmark of the aPf state.

Discussion.—Current experiments for identifying the $\nu = 5/2$ topological order rule out a Pf state by (i) measurements [19,20] of thermal conductance $G^Q = (5/2)\kappa T$ [with temperature T and $\kappa = \pi^2 k_B^2/(3h)$], which is smaller than the Pfaffian prediction $G^Q = (7/2)\kappa T$ and (ii) the observation of upstream modes [22,68], absent for the Pfaffian state. Therefore, the main competitor states are the aPf and phPf. The phPf state is further supported by upstream noise measurements on the interface between $\nu = 5/2$ and integer states [20]. Our proposal to measure conductance plateaus combined with on-plateau shot noise to single out the aPf state, provides a novel, complementary approach to fully identify the $\nu = 5/2$ topological order.

Summary.—We studied $\nu = 5/2$ edge transport in a QPC device. In the incoherent regime, we found that among the Pf, phPf, and aPf candidate states, the aPf uniquely permits *two* mechanisms that generate a conductance plateau at $G = 7/3$. We proposed that on-plateau shot noise, S, differentiate these mechanisms: (i) For $\nu_{QPC} = 3$, which is realized only for the aPf state, S reaches a maximum value $S \approx 0.12 e^3 V/h$ in the experimentally relevant regime (5). (ii) For $\nu_{QPC} = 7/3$, $S \propto \sqrt{\ell^h_{eq}/L_{QPC}}$. We also studied the conductance in the coherent regime, where $G > 5/2$ emerges uniquely for the aPf state, thus providing another fingerprint. Our results pave the way for experimentally pinpointing the $\nu = 5/2$ state in GaAs/AlGaAs, graphene, and further 2D materials. Our approach can be adapted to investigate other even-denominator FQH states.

[1] R. Willett, J. P. Eisenstein, H. L. Störmer, D. C. Tsui, A. C. Gossard, and J. H. English, Observation of an even-denominator quantum number in the fractional quantum Hall effect, Phys. Rev. Lett. **59**, 1776 (1987).

[2] G. Moore and N. Read, Nonabelions in the fractional quantum Hall effect, Nucl. Phys. **B360**, 362 (1991).

[3] C. Nayak, S. H. Simon, A. Stern, M. Freedman, and S. Das Sarma, Non-Abelian anyons and topological quantum computation, Rev. Mod. Phys. **80**, 1083 (2008).

[4] K. K. W. Ma and D. E. Feldman, Partial equilibration of integer and fractional edge channels in the thermal quantum Hall effect, Phys. Rev. B **99**, 085309 (2019).

[5] K. K. W. Ma, M. R. Peterson, V. W. Scarola, and K. Yang, Fractional quantum Hall effect at the filling factor $\nu = 5/2$, in *Encyclopedia of Condensed Matter Physics (Second Edition)* (Academic Press, Cambridge, MA, USA, 2024), Vol. 1, pp. 324–365.

[6] M. Levin, B. I. Halperin, and B. Rosenow, Particle-hole symmetry and the Pfaffian state, Phys. Rev. Lett. **99**, 236806 (2007).

[7] S.-S. Lee, S. Ryu, C. Nayak, and M. P. A. Fisher, Particle-hole symmetry and the $\nu = \frac{5}{2}$ quantum Hall state, Phys. Rev. Lett. **99**, 236807 (2007).

[8] D. T. Son, Is the composite fermion a Dirac particle?, Phys. Rev. X **5**, 031027 (2015).

[9] L. Fidkowski, X. Chen, and A. Vishwanath, Non-Abelian topological order on the surface of a 3d topological superconductor from an exactly solved model, Phys. Rev. X **3**, 041016 (2013).

[10] P. T. Zucker and D. E. Feldman, Stabilization of the particle-hole Pfaffian order by Landau-level mixing and impurities that break particle-hole symmetry, Phys. Rev. Lett. **117**, 096802 (2016).

[11] L. Antonić, J. Vučičević, and M. V. Milovanović, Paired states at 5/2: Particle-hole Pfaffian and particle-hole symmetry breaking, Phys. Rev. B **98**, 115107 (2018).

[12] T. Jolicoeur, Non-Abelian states with negative flux: A new series of quantum Hall states, Phys. Rev. Lett. **99**, 036805 (2007).

[13] X. Wan, Z.-X. Hu, E. H. Rezayi, and K. Yang, Fractional quantum Hall effect at $\nu = 5/2$: Ground states, non-Abelian quasiholes, and edge modes in a microscopic model, Phys. Rev. B **77**, 165316 (2008).

[14] E. H. Rezayi, Landau level mixing and the ground state of the $\nu = 5/2$ quantum Hall effect, Phys. Rev. Lett. **119**, 026801 (2017).

[15] A. C. Balram, M. Barkeshli, and M. S. Rudner, Parton construction of a wave function in the anti-Pfaffian phase, Phys. Rev. B **98**, 035127 (2018).

[16] R. V. Mishmash, D. F. Mross, J. Alicea, and O. I. Motrunich, Numerical exploration of trial wave functions for the particle-hole-symmetric Pfaffian, Phys. Rev. B **98**, 081107 (2018).

[17] M. Yutushui and D. F. Mross, Large-scale simulations of particle-hole-symmetric Pfaffian trial wave functions, Phys. Rev. B **102**, 195153 (2020).

[18] E. H. Rezayi, K. Pakrouski, and F. D. M. Haldane, Stability of the particle-hole Pfaffian state and the 5/2-fractional quantum Hall effect, Phys. Rev. B **104**, L081407 (2021).

[19] M. Banerjee, M. Heiblum, V. Umansky, D. E. Feldman, Y. Oreg, and A. Stern, Observation of half-integer thermal Hall conductance, Nature (London) **559**, 205 (2018).

[20] B. Dutta, V. Umansky, M. Banerjee, and M. Heiblum, Isolated ballistic non-Abelian interface channel, Science **377**, 1198 (2022).

[21] A. K. Paul, P. Tiwari, R. Melcer, V. Umansky, and M. Heiblum, Topological thermal Hall conductance of even denominator fractional states, arXiv:2311.15787.

[22] B. Dutta, W. Yang, R. Melcer, H. K. Kundu, M. Heiblum, V. Umansky, Y. Oreg, A. Stern, and D. Mross, Distinguishing between non-Abelian topological orders in a quantum Hall system, Science **375**, 193 (2022).

[23] J. Park, C. Spånslätt, Y. Gefen, and A. D. Mirlin, Noise on the non-Abelian $\nu = 5/2$ fractional quantum Hall edge, Phys. Rev. Lett. **125**, 157702 (2020).

[24] M. Hein and C. Spånslätt, Thermal conductance and noise of Majorana modes along interfaced $\nu = \frac{5}{2}$ fractional quantum Hall states, Phys. Rev. B **107**, 245301 (2023).

[25] M. Yutushui and D. F. Mross, Identifying non-Abelian anyons with upstream noise, Phys. Rev. B **108**, L241102 (2023).

[26] J. Falson, D. Maryenko, B. Friess, D. Zhang, Y. Kozuka, A. Tsukazaki, J. H. Smet, and M. Kawasaki, Even-denominator fractional quantum Hall physics in ZnO, Nat. Phys. **11**, 347 (2015).

[27] A. A. Zibrov, C. Kometter, H. Zhou, E. M. Spanton, T. Taniguchi, K. Watanabe, M. P. Zaletel, and A. F. Young, Tunable interacting composite fermion phases in a half-filled bilayer-graphene Landau level, Nature (London) **549**, 360 (2017).

[28] J. I. A. Li, C. Tan, S. Chen, Y. Zeng, T. Taniguchi, K. Watanabe, J. Hone, and C. R. Dean, Even-denominator fractional quantum Hall states in bilayer graphene, Science **358**, 648 (2017).

[29] Y. Kim, A. C. Balram, T. Taniguchi, K. Watanabe, J. K. Jain, and J. H. Smet, Even denominator fractional quantum Hall states in higher Landau levels of graphene, Nat. Phys. **15**, 154 (2019).

[30] Q. Shi, E.-M. Shih, M. V. Gustafsson, D. A. Rhodes, B. Kim, K. Watanabe, T. Taniguchi, Z. Papić, J. Hone, and C. R. Dean, Odd- and even-denominator fractional quantum Hall states in monolayer WSe$_2$, Nat. Nanotechnol. **15**, 569 (2020).

[31] K. Huang, H. Fu, D. R. Hickey, N. Alem, X. Lin, K. Watanabe, T. Taniguchi, and J. Zhu, Valley isospin controlled fractional quantum Hall states in bilayer graphene, Phys. Rev. X **12**, 031019 (2022).

[32] Md. S. Hossain, M. K. Ma, Y. J. Chung, S. K. Singh, A. Gupta, K. W. West, K. W. Baldwin, L. N. Pfeiffer, R. Winkler, and M. Shayegan, Valley-tunable even-denominator fractional quantum Hall state in the lowest Landau level of an anisotropic system, Phys. Rev. Lett. **130**, 126301 (2023).

[33] Y. Chen, Y. Huang, Q. Li, B. Tong, G. Kuang, C. Xi, K. Watanabe, T. Taniguchi, G. Liu, Z. Zhu, L. Lu, F.-C. Zhang, Y.-H. Wu, and L. Wang, Tunable even- and odd-denominator fractional quantum Hall states in trilayer graphene, arXiv:2312.17204.

[34] H.-H. Lai and K. Yang, Distinguishing particle-hole conjugated fractional quantum Hall states using quantum-dot-mediated edge transport, Phys. Rev. B **87**, 125130 (2013).

[35] C. Spånslätt, J. Park, Y. Gefen, and A. D. Mirlin, Conductance plateaus and shot noise in fractional quantum Hall point contacts, Phys. Rev. B **101**, 075308 (2020).

[36] F. D. M. Haldane, Fractional quantization of the Hall effect: A hierarchy of incompressible quantum fluid states, Phys. Rev. Lett. **51**, 605 (1983).

[37] B. I. Halperin, Statistics of quasiparticles and the hierarchy of fractional quantized Hall states, Phys. Rev. Lett. **52**, 1583 (1984).

[38] A. H. MacDonald, Edge states in the fractional-quantum-Hall-effect regime, Phys. Rev. Lett. **64**, 220 (1990).

[39] See Supplemental Material at http://link.aps.org/supplemental/10.1103/PhysRevLett.132.256601 which includes details on (i) a summary of the key features of incoherent transport along FQH edges, (ii) the derivation of the conductance plateau formula (1), (iii) shot noise characteristics for the aPf state, (iv) the derivation of Eq. (9), (v) an RG analysis near the two fixed points for the aPf edge attached to leads, (vi) the derivation of the two-terminal conductance G [Eq. (10)] for the QPC geometry (cf. Fig. 2) in the coherent regime, (vii) the permitted range of G, and (viii) the derivation of a Kubo formula for the conductance. The Supplemental Material also includes Refs. [40–42].

[40] I. Protopopov, Y. Gefen, and A. Mirlin, Transport in a disordered $\nu = 2/3$ fractional quantum Hall junction, Ann. Phys. (Amsterdam) **385**, 287 (2017).

[41] C. Nosiglia, J. Park, B. Rosenow, and Y. Gefen, Incoherent transport on the $\nu = 2/3$ quantum Hall edge, Phys. Rev. B **98**, 115408 (2018).

[42] C. L. Kane and M. P. A. Fisher, Thermal transport in a Luttinger liquid, Phys. Rev. Lett. **76**, 3192 (1996).

[43] J. Nakamura, S. Liang, G. C. Gardner, and M. J. Manfra, Half-integer conductance plateau at the $\nu = 2/3$ fractional quantum Hall state in a quantum point contact, Phys. Rev. Lett. **130**, 076205 (2023).

[44] M. H. Fauzi, K. Nakagawara, K. Hashimoto, N. Shibata, and Y. Hirayama, Synthesizing $2h/e^2$ resistance plateau at the first Landau level confined in a quantum point contact, Commun. Phys. **6**, 1 (2023).

[45] J. Yan, Y. Wu, S. Yuan, X. Liu, L. N. Pfeiffer, K. W. West, Y. Liu, H. Fu, X. C. Xie, and X. Lin, Anomalous quantized plateaus in two-dimensional electron gas with gate confinement, Nat. Commun. **14**, 1 (2023).

[46] A. Bid, N. Ofek, M. Heiblum, V. Umansky, and D. Mahalu, Shot noise and charge at the 2/3 composite fractional quantum Hall state, Phys. Rev. Lett. **103**, 236802 (2009).

[47] R. Bhattacharyya, M. Banerjee, M. Heiblum, D. Mahalu, and V. Umansky, Melting of interference in the fractional quantum Hall effect: Appearance of neutral modes, Phys. Rev. Lett. **122**, 246801 (2019).

[48] S. Biswas, R. Bhattacharyya, H. K. Kundu, A. Das, M. Heiblum, V. Umansky, M. Goldstein, and Y. Gefen, Shot noise does not always provide the quasiparticle charge, Nat. Phys. **18**, 1476 (2022).

[49] T. Giamarchi and H. J. Schulz, Anderson localization and interactions in one-dimensional metals, Phys. Rev. B **37**, 325 (1988).

[50] J. Park, A. D. Mirlin, B. Rosenow, and Y. Gefen, Noise on complex quantum Hall edges: Chiral anomaly and heat diffusion, Phys. Rev. B **99**, 161302 (2019).

[51] C. Spånslätt, J. Park, Y. Gefen, and A. D. Mirlin, Topological classification of shot noise on fractional quantum Hall edges, Phys. Rev. Lett. **123**, 137701 (2019).

[52] R. A. Melcer, B. Dutta, C. Spånslätt, J. Park, A. D. Mirlin, and V. Umansky, Absent thermal equilibration on fractional quantum Hall edges over macroscopic scale, Nat. Commun. **13**, 1 (2022).

[53] R. Kumar, S. K. Srivastav, C. Spånslätt, K. Watanabe, T. Taniguchi, Y. Gefen, A. D. Mirlin, and A. Das, Observation of ballistic upstream modes at fractional quantum Hall edges of graphene, Nat. Commun. **13**, 1 (2022).

[54] S. Manna, A. Das, M. Goldstein, and Y. Gefen, Full classification of transport on an equilibrated 5/2 edge via shot noise, Phys. Rev. Lett. **132**, 136502 (2024).

[55] S. Manna, A. Das, and M. Goldstein, Shot noise classification of different conductance plateaus in a quantum point contact at the $\nu = 2/3$ edge, arXiv:2307.05175.

[56] C. Spånslätt, Y. Gefen, I. V. Gornyi, and D. G. Polyakov, Contacts, equilibration, and interactions in fractional quantum Hall edge transport, Phys. Rev. B **104**, 115416 (2021).

[57] F. Lafont, A. Rosenblatt, M. Heiblum, and V. Umansky, Counter-propagating charge transport in the quantum Hall effect regime, Science **363**, 54 (2019).

[58] Y. Cohen, Y. Ronen, W. Yang, D. Banitt, J. Park, M. Heiblum, A. D. Mirlin, Y. Gefen, and V. Umansky, Synthesizing a $\nu = 2/3$ fractional quantum Hall effect edge state from counter-propagating $\nu = 1$ and $\nu = 1/3$ states, Nat. Commun. **10**, 1920 (2019).

[59] M. Hashisaka, T. Jonckheere, T. Akiho, S. Sasaki, J. Rech, T. Martin, and K. Muraki, Andreev reflection of fractional quantum Hall quasiparticles, Nat. Commun. **12**, 1 (2021).

[60] M. Hashisaka, T. Ito, T. Akiho, S. Sasaki, N. Kumada, N. Shibata, and K. Muraki, Coherent-incoherent crossover of charge and neutral mode transport as evidence for the disorder-dominated fractional edge phase, Phys. Rev. X **13**, 031024 (2023).

[61] S. H. Simon and B. Rosenow, Partial equilibration of the anti-Pfaffian edge due to Majorana disorder, Phys. Rev. Lett. **124**, 126801 (2020).

[62] K. K. W. Ma and D. E. Feldman, Thermal equilibration on the edges of topological liquids, Phys. Rev. Lett. **125**, 016801 (2020).

[63] H. Asasi and M. Mulligan, Partial equilibration of anti-Pfaffian edge modes at $\nu = 5/2$, Phys. Rev. B **102**, 205104 (2020).

[64] S. K. Srivastav, R. Kumar, C. Spånslätt, K. Watanabe, T. Taniguchi, A. D. Mirlin, Y. Gefen, and A. Das, Vanishing thermal equilibration for hole-conjugate fractional quantum Hall states in graphene, Phys. Rev. Lett. **126**, 216803 (2021).

[65] G. Le Breton, R. Delagrange, Y. Hong, M. Garg, K. Watanabe, T. Taniguchi, R. Ribeiro-Palau, P. Roulleau, P. Roche, and F. D. Parmentier, Heat equilibration of integer and fractional quantum Hall edge modes in graphene, Phys. Rev. Lett. **129**, 116803 (2022).

[66] S. K. Srivastav, R. Kumar, C. Spånslätt, K. Watanabe, T. Taniguchi, A. D. Mirlin, Y. Gefen, and A. Das, Determination of topological edge quantum numbers of fractional quantum Hall phases by thermal conductance measurements, Nat. Commun. **13**, 1 (2022).

[67] G. Li, A. Luican-Mayer, D. Abanin, L. Levitov, and E. Y. Andrei, Evolution of Landau levels into edge states in graphene, Nat. Commun. **4**, 1744 (2013).

[68] A. Bid, N. Ofek, H. Inoue, M. Heiblum, C. L. Kane, V. Umansky, and D. Mahalu, Observation of neutral modes in the fractional quantum Hall regime, Nature (London) **466**, 585 (2010).